ORIGINAL ARTICLE

A C G publications

Org. Commun. 15:2 (2022) 184-203

organic communications

Chemical descriptors, PASS, molecular docking, molecular dynamics and ADMET predictions of glucopyranoside derivatives as inhibitors to bacteria and fungi growth

Sarkar M. A. Kawsar [1,*], Ajoy Kumer [2], Nasrin S. Munia [1]

Mohammed A. Hosen [1], Unesco Chakma [3] and Shopnil Akash [4]

[1]*Laboratory of Carbohydrate and Nucleoside Chemistry, Department of Chemistry, Faculty of Science, University of Chittagong, Chittagong, Bangladesh*

[2]*Department of Chemistry, European University of Bangladesh, Gabtoli, Dhaka-1216, Bangladesh*

[3]*Department of Electrical and Electronics Engineering, European University of Bangladesh, Gabtoli, Dhaka-1216, Bangladesh*

[4]*Department of Pharmacy, Daffodil International University, Sukrabad, Dhaka-1207, Bangladesh*

(Received March 25, 2022; Revised April 09, 2022; Accepted April 10, 2022)

Abstract: The methyl α-D-glucopyranoside and its derivatives have been estimated as the antimicrobial agents against numerous human pathogens, which is constantly amplifying the attention of medicinal chemists to design new bioactive molecules and their structure-activity relationship (SAR) while the computational tools are the most lucid and trustable avenue to perform their theoretical profile building up. Firstly, the predictionof activity spectra for substances (PASS) value has illustrated initially information about the antifungal, antibacterial, antiviral, and anticancer potential. It was observed that the PASS predicted pathogens supported their score higher in fungal species than bacteria. However, the "Lipinski five rule" has been monitored for drug-likeness properties. After confirming their biological significance, molecular docking has been completed against both the bacteria and fungi and these docked complexes have been optimized for molecular dynamics through the water system. A molecular docking study against nine bacterial and fungal pathogens revealed promising binding affinity and non-bonding interaction mostly for derivatives (**5-8**). The chemical descriptors have been obtained using the density functional theory (DFT) and predict their chemical stability and softness in the biological system. The molecular dynamics study was found to be the best stability of all docked complexes. At last, the ADMET properties have been calculated and provide the safe use and non-carcinogenic fact with low toxicity for both aquatic and non-aquatic species. Finally, it is concluded that these selected derivatives (**5-8**) are highly antifungal potential molecules than antibacterial potential which has been varied with respect to their structural side chain in the D-glucopyranoside sequence.

Keywords: Chemical stability; pass prediction; molecular dynamics; DFT calculation; ADMET. © 2022 ACG Publications. All rights reserved.

1. Introduction

The carbohydrates have been recognized and rewarded as the cardinal components of balanced diet dietary fibre[1] and obtained from plants[2] which have been involved in the photosynthesis procedure as forming in the plant body.[3] In the addition, the energy in the human diet is mostly obtained from

* Corresponding author: E-Mail: akawsar@cu.ac.bd; Tel.: +88-01762717081

The article was published by ACG Publications
http://www.acgpubs.org/journal/organic-communications © April-June 2022 EISSN:1307-6175
DOI:http://doi.org/10.25135/acg.oc.122.2203.2397
Available online: April 20, 2022

carbohydrates[4], nearing 50–70% of total energy consumption and burn in the human body to produce energy and carbon dioxide for use in the human physiological system,Energy source, structural building components of genetic material, identification of the cell surface, signal transduction, the spread of the tumour, depression and other affective disorders[5]. In addition, it maintains body weight and blood lipid and human metabolism[6]. Besides having in vast functional activities living body, it has been enlarged as drug and therapeutic compounds with its structural modification[7] acted as carbohydrate-based cancer therapeutics[8], glycomimetic drugs[9],micro/nanocapsules[10], antimicrobial drugs[11], antiviral potential drugs[12], antibiotic.[13]Regarding that case, carbohydrate has to be acquainted with the crucial components of a living body, and it could be got hold of as the form of sugars, starch, and non-starch polysaccharide.[14] It is reported that methyl α-D-glucopyranoside is a derivative from carbohydrates (www.ebi.ac.uk/chebi/chebiOntology) including the group of sugars. Many scientists have been reported that this derivative (methyl α-D-glucopyranoside) consists of a wide variety of antifungal[15], antibacterial[16], anticancer properties[17], antiviral and SARS-CoV-2.[18] Due to having the vast attention as potential molecules for drug design, the methyl α-D-glucopyranoside and its derivateshave been selected to evaluate the biological significance against various human pathogens using computational tools.

Carbohydrates are the most available biomolecules belonging to organic compounds class. They come from living organism's kingdom. Around the world, scientists are investing in medicinal research to find more effective and safer antimicrobial agents for the treatment of diseases caused by pathogenic organisms. For a long time, carbohydrates remained an attractive research subject for scientists due to the important role played in the functioning of biological systems, namely the growth and proliferation of cells, communication between cells and the immune response. They are also the source of metabolic energy supply and responsible for the fine-tuning of cell-cell interactions and many other important biological processes .Other advantages of carbohydrates also pointed out are the numerous and diverse biological activities which they exert against pathogenic germs. Among biological activities, we can quote antibacterial, antiviral, antineoplastic, antiprotozoal, and antifungal activities.

Since these glucopyranoside compounds have been studied experimentally previously by Kawsar et al. 2009[19] by following a reaction scheme by the treatment of myristoyl chloride and acylating agent as shown in Figure 1. The following pathogens are taken for this study. *Salmonella enterica* (PDB ID: 4W4M) is the most familiar Gram-negative bacterial infection and consists of a variety of strains.[20] An important characteristic of all deadly Salmonella strains is Salmonella Pathogenicity Islands (SPIs) which are observed in all bacterial organisms of Salmonella.[21]*Francisella tularensis* (PDB ID: 3TQV); Francisella tularensis has been categorized as a group "A" restricted poison. There is presently no FDA-approved antagonist that precisely inhibits this infection (Francisella tularensis).Tularemia is generally treated with only a few medicines, like fluoroquinolones.[22]*Helicobacter pylori* (PDB ID: 5J1L); approximately half of the world's population is infected with Helicobacter pylori which is a Gram-negative bacteria that can cause stomach ulcers, a significant cause of stomach.[23]*Pneumocystis carinii* (DB ID: 4IXE); Pneumocystis pneumonia, or PCP, is a fungal disease of the lungs. Patients with a weakened immune system, like those with AIDS, are more susceptible to it.[24]This infection has been carried along by *Pneumocystis jirovecii*, a yeast-like fungus (PJP).[25]*Coccidioides immitis* (PDB ID: 1D2K); Coccidioides which has been known as metabolizing genes, membrane-related proteins, and supposedly pathogenic materials have developed as a result of contact with an animal host. When *Coccidioides immitis* infects a person, it can lead to coccidioidomycosis (valley fever). *Cryptococcus neoformans*(PDB ID: 6KO6); *Cryptococcus neoformans* has been considered the most familiar fungus that may be found in the environment all over the globe. When inhaling the tiny fungi, anyone can become affected with *C. neoformans*, however, most people who are susceptible to it never get affected.[26] The majority of instances of *C. neoformans* disease happen in people with weakened immune systems, like those with severe HIV/AIDS.[27]*Candida albicans* (PDB ID:4YDE). Candida species, which have been typically found in the vulvovaginal flora, under certain environments, aggressive infections can occur, weakening the host's immune function.[28]

It is reiterated that the glucopyranoside derivatives have reported antibacterial and antifungal properties[29-36] so that this study conveys the various chain effects in replacing the R group (shown in Figure 1). For that case, the various computational parameters, such as molecular docking, ADME parameters, MD, QSAR data and PlogIC50, Lipinski rule, pharmacokinetics and drug-likeness, aquatic and non-aquatic toxicity have been investigated with respect to the various chains.

2. Experimental

2.1. Optimization and Ligand Preparation

Utilizing DFT functional, molecular optimization has been performed from the DMol code of Material Studio 08.[37] The highly precise result is obtained while in DMol code, the B3LYP functional and 6-31G++ was set up properly due to the presence of the electronegative atom, oxygen. After the optimization is properly performed, these optimized lead compounds were then exported as pdb files for further computational investigation such as molecular docking, molecular dynamic and ADMET.Gibbs free energy, dipole moment, enthalpy, heat capacity, entropy, total energy, and polarizability were calculated for each compound. Electronic molecular orbital properties HOMO and LUMO were calculated based on the same geometrical theory. HOMO-LUMO energy gap, molecular hardness (η), and molecular softness (*S*) were calculated for each ester from energy values of electronic orbitals HOMO and LUMO, based on Parr and Pearson's explanation of DFT and Koopmans' theorem on the interrelation between ionization energy and electronic energy (E), electron affinity (*A*), and ionization potential (*I*) with HOMO and LUMO energies (ε). The following equations were used to calculate global chemical reactivity by analyzing molecular orbital features.

$$\text{Gap } (\Delta\varepsilon) = \varepsilon\text{LUMO} - \varepsilon\text{HOMO}$$

$$\eta = \frac{[\varepsilon\text{LUMO} - \varepsilon\text{HOMO}]}{2}$$

$$S = \frac{1}{\eta}$$

$$\mu = \frac{[\varepsilon\text{LUMO} + \varepsilon\text{HOMO}]}{2}$$

$$\chi = -\frac{[\varepsilon\text{LUMO} + \varepsilon\text{HOMO}]}{2}$$

$$\omega = \frac{\mu 2}{2\eta}$$

2.2. Pass Prediction

Pass prediction value or Pa>Pi value is one of the major properties of a biologically active compound. To get the pass prediction value, PASS online tools, "http://way2drug.com/PassOnline/predict.php". This website provides a wide variety of Prediction information such as antiviral, antibacterial, antifungal and anticancer etc.[38]This server can predict >4000 types of antimicrobial function, together with drug and non-drug activity, leading to suggestion of best potential objects with 90% validity. PASS calculation outcomes are expressed as Pa (probability of active molecule) and Pi (probability of inactive molecule). Pa and Pi scores range from 0.00 to 1.00, and usually, Pa + Pi ≠ 1, since these probabilities are calculated independently. Biological activities for which Pa > Pi are considered probable only for a selected drug molecule.

2.3. Lipinski Rule and Pharmacokinetics

The data of Lipinski Rule is obtained from SWISADMETSAR online web which is the trusted website[39] "http://www.swissadme.ch/index.php" for getting different pharmacokinetic properties Lipinski Rule is one of the major pharmacokinetics parameters of any bioactive compound. Although different values of the molecules are shown in the Table (2 &Supp.), it is further explained in their suitability in the discussion section. Traditionally, therapeutics have been small molecules that fall within the Lipinski's rule of five (i.e., a molecule with a molecular mass less than 500 Da, no more than 5 hydrogen bond donors, no more than 10 hydrogen bond acceptors, and an octanol–water partition coefficient log P not greater than 5).

2.4. Protein preparation

First, we searched the Protein Data Bank website on Google and enter the Protein Data Bank (PDB) website "https://www.rcsb.org " Then the experimental of Protein were downloaded from Protein *Data Bank in the format of PDB. While the four was bacteria strain, such as Salmonella enterica* (4W4M), *Francisella tularensis* (3TQV), *Helicobacter pylori* (5J1L), *Salmonella typhi* (3UU2) and six was a fungal strain, for instance, *Aspergillus niger* (1ACZ), *Aspergillus niger* (1KUM), *Pneumocystis carinii* (4IXE), *Coccidioides immitis* (1D2K), *Cryptococcus neoformans* (6KO6), *Candida albicans* (4YDE). Swiss-Pdb viewer software (version 4.1.0) was employed for energy minimization of the protein.The molecules of water and excess ligand, which was previously attached with protein, have been cleaned using Pymol software 3 (https://pymol.org/2/)[40] and obtained the raw protein strain for molecular docking.

2.5. Molecular Docking Study and Visualization

For molecular docking, the virtual screening tools (PyRx) was exercised.[41]The grid center was points at X = − 0.0130, Y = − 1.1682, Z = 0.7164, and the dimension (Å) X = 30.8323, Y = 47.5945, Z = 30. 5023. The uploaded protein and ligand were selected in autodockvina wizard from PyRx software for docking and binding affinity was recorded from this simulation. Using grid box, wrap the protein's substrate-binding region and non-covalent interaction between the ligands and protein were determined with the help of BIOVIA Discovery Studio Visualizer.

2.6. Molecular Dynamics

MD simulations have been completed with the help of NAMD software in high configuration computer-based their binding energy computer.[42]The highest ligand-protein interaction up to 100 ns for holo-form (drug-protein) was validated utilizing MD simulation by using AMBER14 protective shield.[43]Employing 0.9 percent NaCl at 298 K, the system was pretreated in the addition of distilled water. Åacross every part of the operation and cover the periodic during the simulation, the RMSD and RMSFutilizing VMD program after the simulation was obtained.

2.7. ADMET Properties

To know the pharmacokinetic properties of the ligand molecules for therapeutic performance or bioactivity, the ADMET investigations play a crucial role. The parameters of ADMET Data have been collected via the amdetSAR "http://lmmd.ecust.edu.cn/admetsar2" which has been established as the most popular database for predicting the AMDET parameters.[44] The major pharmacokinetics properties which we find out by ADMET studies include plasma protein binding, Human intestinal absorption, Caco-2 permeability, blood-brain barrier, renal organic cation transporter, CYP450 2C9 substrate.

3. Results and Discussion

3.1. Chemistry

By performing the structural activity relationship (SAR) of glucose, we synthesized a derivative of glucose which is methyl α-D-glucopyranoside[45-47] (Figure 1). We then draw the structure of methyl α-D-glucopyranoside for further study and completed it using the DFT function of material Studio 08. Then the reported structures are taken and performed the asymmetry and geometry calculation. These glucopyranoside derivative structures are then studied by various parameters in the computational and biological activity.

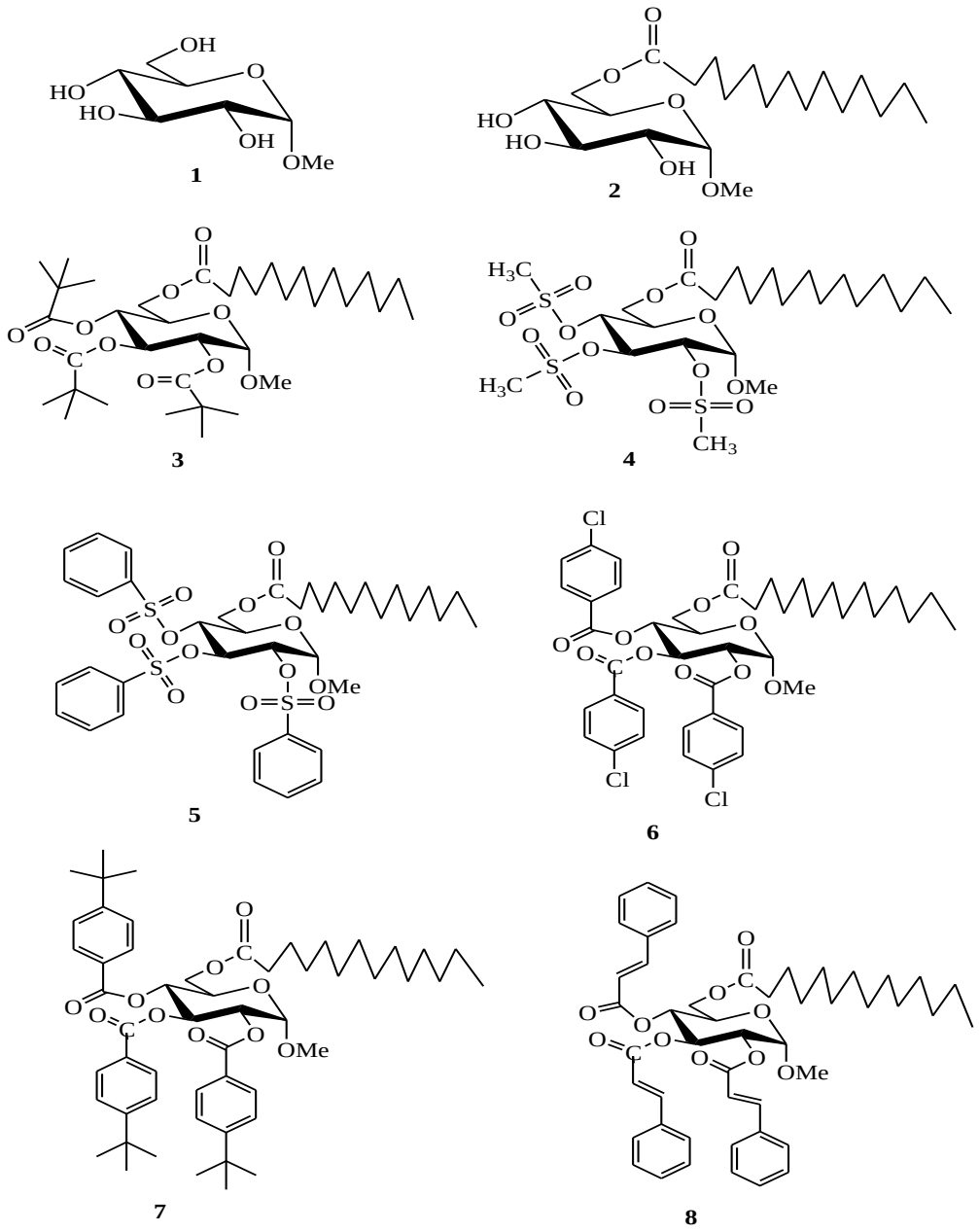

Figure 1. Structure of the synthesized methyl α-D-glucopyranoside and its derivatives

3.2. Optimized Structure of the Tested Ligand

The binding assays with genetic material, in a first set of experiments, were performed using the produced ligands' chemical characteristics were further examined using the DFT method for their quantum calculation and their geometry optimization. The optimized geometrical structure of all synthesized compounds is mentioned below (Figure 2).

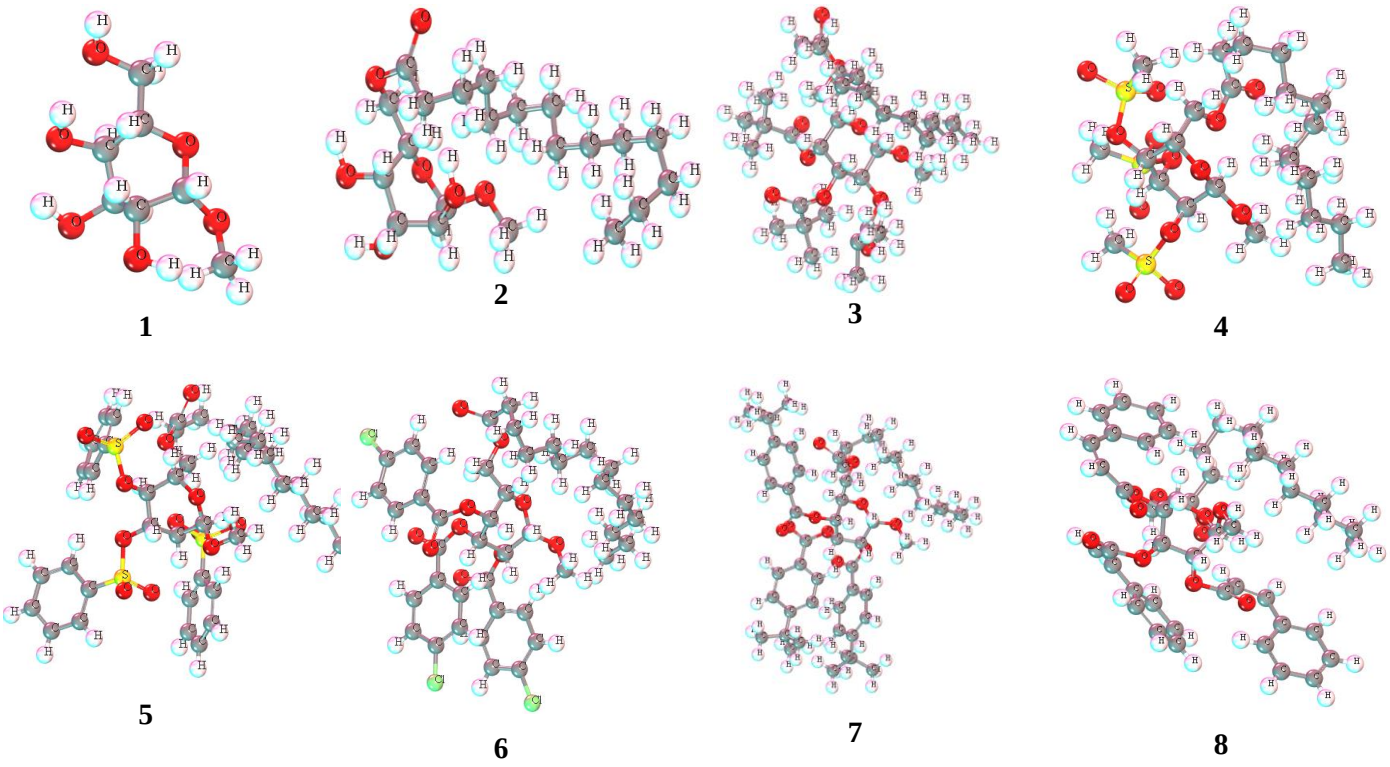

Figure 2. The optimized geometrical structure of ligands

3.3. Evaluation of FTIR and UV-Vis Spectra of Compounds

One of the most commonly employed methods that have been applied to detect organic and polymeric elements is Fourier transform infrared analysis (FTIR).[48] This approach employs infrared light to inspect test materials and assess their chemical characteristics through using the FTIR analysis method. The FTIR system transmits infrared light of approximately 10,000 to 100 cm-1 through a material, with some energy consumed and some escaping through. Signals from analyzers normally range from 4000 cm-1 to 400 cm^{-1} which reflect the molecular fingerprint of the sample.[49]

Table 1. FTIR frequency range (cm^{-1}) of the glucopyranoside derivatives

Entry	Frequency range (cm^{-1}) and functional group present
1	2400 cm^{-1}, 2500 cm^{-1}, 2800 cm^{-1} (C-H), 2900 cm^{-1} (C-H)
2	1000 cm^{-1},1200 cm^{-}1,1900 cm^{-1}, 2500 cm^{-1}, 2600 cm^{-1}, 2800 cm^{-1} (C-H)
3	1000 cm^{-1},1200 cm^{-1}, 1300 cm^{-1}, 1350cm^{-1}, 2300cm^{-1}, 2400 cm^{-1}, 2600 cm^{-1} and 2900 cm^{-1} (C-H)
4	2300 cm^{-1} (C–O), 2500 cm^{-1} and 2800 cm^{-1}(C-H)
5	1000 cm^{-1}, 2400 cm^{-1}, 2500 cm^{-1} and 2800 cm^{-1}(C-H)
6	1000 cm^{-1},1400 cm^{-1}, 2500 cm^{-1}, 2700 cm^{-1} and 2900 cm^{-1} (C-H)
7	1300 cm^{-1},2600 cm^{-1} and 2800 cm^{-1} (C-H)
8	2500 cm^{-1}, 2600 cm^{-1},2800 cm^{-1} (C-H)

For compounds **1**, the FTIR frequency region has been displayed (Table 1 and Figure 3) 2400 cm^{-1} while the compounds 2 provided six peaks at 1000 cm^{-1},1200 cm^{-1},1900 cm^{-1}, 2500 cm^{-1}, 2600 cm^{-1} 2800 cm^{-1} (C-H), compound 3 provided 1000 cm^{-1}, 1200 cm^{-1}, 1300 cm^{-1}, 2400 cm^{-1}, 2600 cm^{-1}

and 2800 cm^{-1}(C-H), compound 4 exhibited 2300 cm^{-1} and 2800 cm^{-1}, 2300 cm^{-1} (C–O), 2500 cm^{-1} and 2800 cm^{-1} (C-H), compound 5 gave the 1000 cm^{-1},2400 cm^{-1}, 2500 cm^{-1},and 2800 cm^{-}1, compound 6 showed 1000 cm^{-1}, 1400 cm^{-1}, 2500 cm^{-1}, 2700 cm^{-1} and 2900 cm^{-1}, compound 7 provided 1300 cm^{-1}, 2600 cm^{-1} and 2800 cm^{-1} and the compound 8 has been reported 2500 cm^{-1}, 2600 cm^{-1},and 2800 cm^{-1} FTIR region. UV-Vis spectrum are presented in the Figure 4.

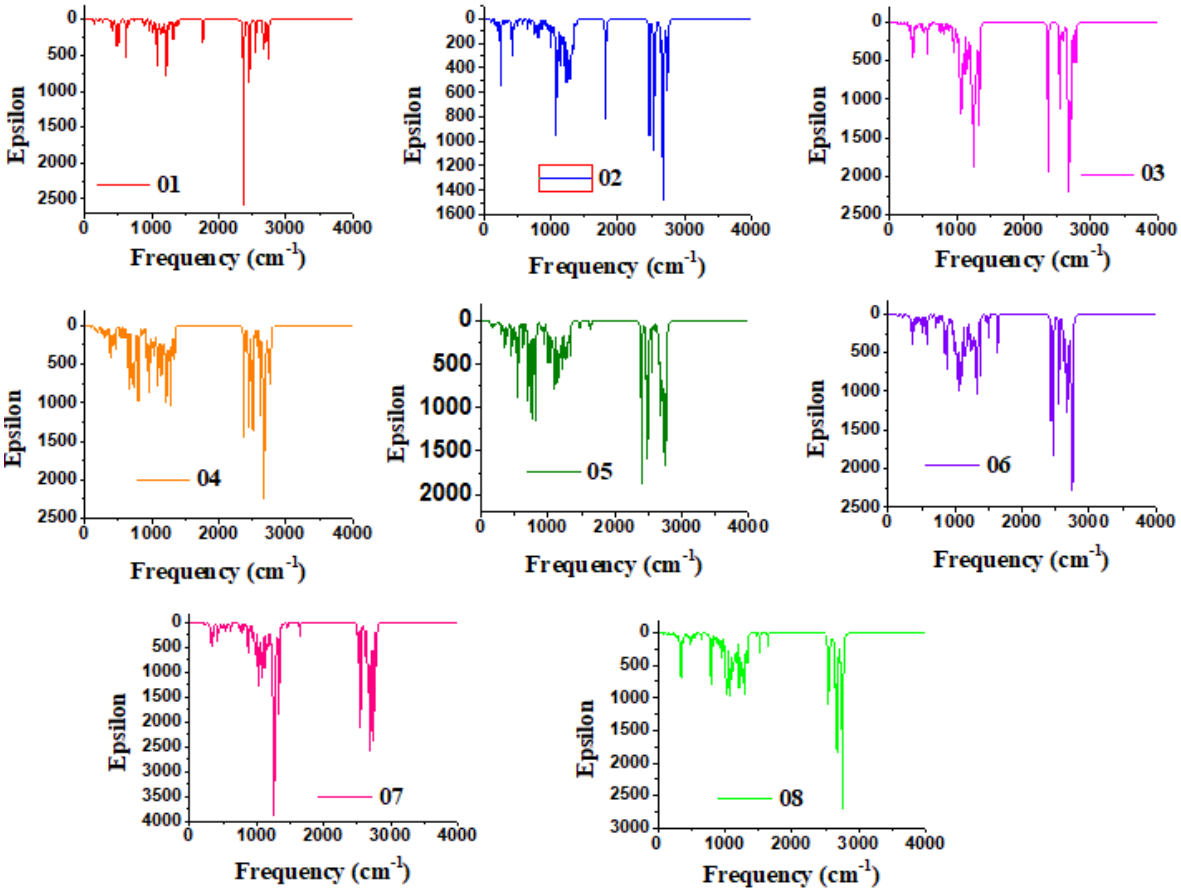

Figure 3. FTIR spectrum of the **1-8** compounds by the computational calculation

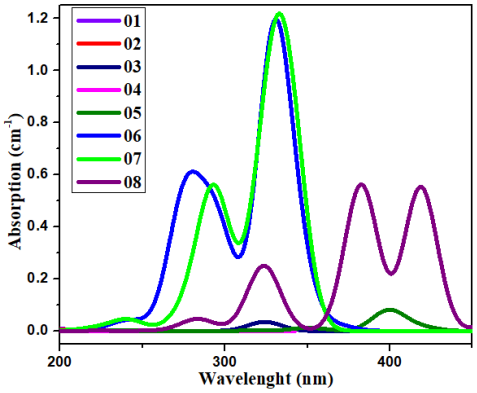

Figure 4. UV-Vis spectrum by the computational calculation

The UV-visible spectroscopy using Time-dependent density functional theory method is a benchmark for the molecular orbital analysis of fused aromatic ring-system, ensuring the balance between accuracy and computational expense. Each of the two characteristic electronic transition states

from the derivatives is presented in Figure4. In this study, kinetic stability and reactive sites depend on the first electronic transition from the ground state (S_0) to singlet (S_1). Derivatives **6** and **7**which are having 4-chlorobenzoyl and 4-tert-butylbenzoyl ringshow broad absorption bands at 345.16 nm along with their absorptionvalue1.2 cm^{-1}. Moreover, derivative **8** exhibit broad absorption bands at 386.27 nm and 430.61 nm along with their absorption value 0.5 cm^{-1}. Both of the broadband absorption wavelengths at 345.16 nm with the highest intensities are mainly due to the electronic transition from HOMO to LUMO. HOMO's electron density focuses C-C double bonds (pi-electrons) in both rings. The lower energy of excitation corresponding to the HOMO-LUMO energy gap maximizes the chemical reactivity and minimizes kinetic stability.

3.4. Lipinski Rule, Pharmacokinetics and Drug-likeness

Drug characteristics of the features of bioactive molecules, such as membrane permeability, GI absorption and bioavailability, partition coefficient (logP), molecular weight (MW) and a number of hydrogen bond acceptors/donors provide overall information of chemical acceptances and drug-likeness in view of Lipinski rule.[50] It is found the first three compounds (**1**,**2**, **3**) completely fulfill all the criteria after further study and computational analysis. But, the other five compounds do not fulfill all criteria due to high molecular weight. That's why we want to see how much biological activity shows these mentioned compounds by neglecting molecular weight and we go a better result which full 80% of criteria. The result has been given below Table 2.

Table 2. Data of Lipinski rule, pharmacokinetics and drug-likeness

	Properties										
Entry	**NBR**	**HBA**	**HBD**	**TPSA, Å²**	**Consensus Log Po/w**	**Log Kp (skin permeation), cm/s**	**Lipinski rule** Result	violation	**MW**	**Bioavailability Score**	**GI absorption**
1	02	06	04	99.38	1.76	-9.37	Yes	0	194.18	0.55	Low
2	16	07	03	105.45	3.13	-5.78	Yes	0	404.54	0.55	High
3	25	10	0	123.66	7.28	-3.11	Yes	1	656.89	0.55	Low
4	22	13	0	200.00	3.86	-6.98	No	2	638.81	0.17	Low
5	25	13	0	200.01	7.18	-4.17	No	3	825.02	0.17	Low
6	25	10	0	123.66	9.48	-2.22	No	2	820.19	0.17	Low
7	28	10	0	123.66	11.4	-0.39	No	2	885.18	0.17	Low
8	28	10	0	123.66	8.68	-2.49	No	2	794.97	0.17	Low

3.5. PASS Prediction

It seems that a large number of research projects does not reach the final stage because severe unfavorable side effect and toxicity are unknown and this unfavorable effect found or arise far too late. But, today in this modern age, it is possible to predict more than 3678 pharmacological effects, modes of action, carcinogenicity, teratogenicity and other biological properties of compounds using easy computer software called PASS and predict.[51]Although the data, which is illustrated from pass prediction, is not so good this is expected. However, some scientist has reported that these compound derivatives consist of antifungal and antibacterial properties in their literatures[52]It can be seen in **Table 3** that the derivatives **2–8** showed $0.36 < Pa < 0.53$ for antibacterial, $0.09 < Pa < 0.38$ for antifungal $0.02 < Pa < 0.31$ for antibiotic, $0.19 < Pa < 0.42$ for anticancer and $0.19 < Pa < 0.71$ for antiviral. These results reveal that these molecules were more efficient against bacterial and virus pathogens in comparison with fungal pathogens. The attachment of additional aliphatic acyl chainincreased antibacterial activity (3, Pa = 0.534) (8, Pa = 0.534) of (1, Pa = 0.614), whereas the insertion of other aromatic groups decreased the

activity somewhat. The same scenario was observed for antifungal, antiviral and anticancer activity, where acyl chain analogs revealed improved values compared to the benzoyl analogs. However, derivative **2**, which have the myristoyl group, exhibited the highest antiviral activities. An attempt was also made to predict the antibiotic parameters of these derivatives.

Table 3. Data of PASS prediction.

Predictions of different parameters										
Entry	**Antiviral**		**Antibacterial**		**Antifungal**		**Antibiotic**		**Anticancer**	
	Pa	Pi	Pa	Pi	Pa	Pi	Pa	Pi	Pa	Pi
1	0.765	0.004	0.614	0.016	0.123	0.020	0.046	0.006	0.514	0.010
2	0.718	0.005	0.528	0.014	0.113	0.033	0.025	0.010	0.422	0.020
3	0.451	0.018	0.534	0.013	0.101	0.062	0.313	0.013	0.418	0.021
4	0.392	0.039	0.408	0.028	0.112	0.035	0.079	0.015	0.196	0.090
5	0.417	0.073	0.369	0.038	0.384	0.053	0.233	0.025	0.307	0.022
6	0.191	0.098	0.470	0.019	0.106	0.049	0.022	0.011	0.404	0.022
7	0.603	0.013	0.470	0.019	0.094	0.090	0.257	0.019	0.416	0.021
8	0.536	0.018	0.538	0.013	0.097	0.077	0.289	0.015	0.224	0.136

3.6. Chemical descriptors

Molecular orbitals provide valuable information about electronic structure.[53] Using the DFT method, the energy values of the highest occupied and lowest unoccupied molecular orbitals have been calculated. Molecules with a less orbital gap seem to be more polar in nature, have a lower efficacy where the highest E (gap) represent the highest stability and are considered as softer molecules.[54] The chemical potential (m), hardness (h), softness (S) and electrophilicity coefficient (u) help to determine the biological activity of lead compound.[55,56] Secondly, chemical potential, the positive chemical potential mainly related to stability and when the softness is lower than hardness, this means the compounds is highly stable.[57,58] The overall Frontier Molecular Orbitals (HOMO, LUMO) value is given below Table 4.

Table 4 . Energy (eV) of chemical descriptors

Chemical descriptors								
S/N	**A=-LUMO**	**I= HOMO**	**Energy =I-A**	**Chemical potential** $(\mu) = -\frac{I+A}{2}$	**Electronegativity** $(\chi) = \frac{I+A}{2}$	**Hardness** $(\eta) = \frac{I-A}{2}$	**Softness** $(\sigma) = \frac{1}{\eta}$	**Electrophilicity** $(\omega) = \frac{\mu^2}{2\eta}$
1	-1.021	-10.407	9.386	5.714	-5.714	-4.693	-0.2131	-3.4786
2	-0.858	-10.428	9.570	5.643	-5.643	-4.785	-0.2090	-3.3274
3	-2.036	-9.222	7.186	5.629	-5.629	-3.593	-0.2783	-4.4094
4	-3.911	-9.982	6.071	6.9465	-6.9465	-3.0355	-0.3294	-7.9483
5	-2.884	-9.364	6.48	6.124	-6.124	-3.24	-0.3086	-5.7876
6	-1.824	-9.017	7.193	5.4205	-5.4205	-3.5965	-0.2780	-4.0848
7	-1.441	-8.641	7.20	5.041	-5.041	-3.60	-0.2778	-3.5294
8	-1.449	-8.309	6.86	4.879	-4.879	-3.43	-0.2915	-3.4701

Compound (**4**) had the highest softness value and lowest values for HOMO-LUMO energy gap (6.071 eV) and hardness, indicating reactivity much greater than that of the other compounds, according to the criteria of Pearson. Compound (**2**) had the highest energy gap (9.570eV), and this value was higher than that of parent compound (**1**) (9.386eV), indicating that these two compounds had similar stability.

3.7. Frontier Molecular Orbitals (HOMO and LUMO)

For better comprehension, Figure 5 represents the frontier orbital illustration of HOMO and LUMO marking by colored uniquely.

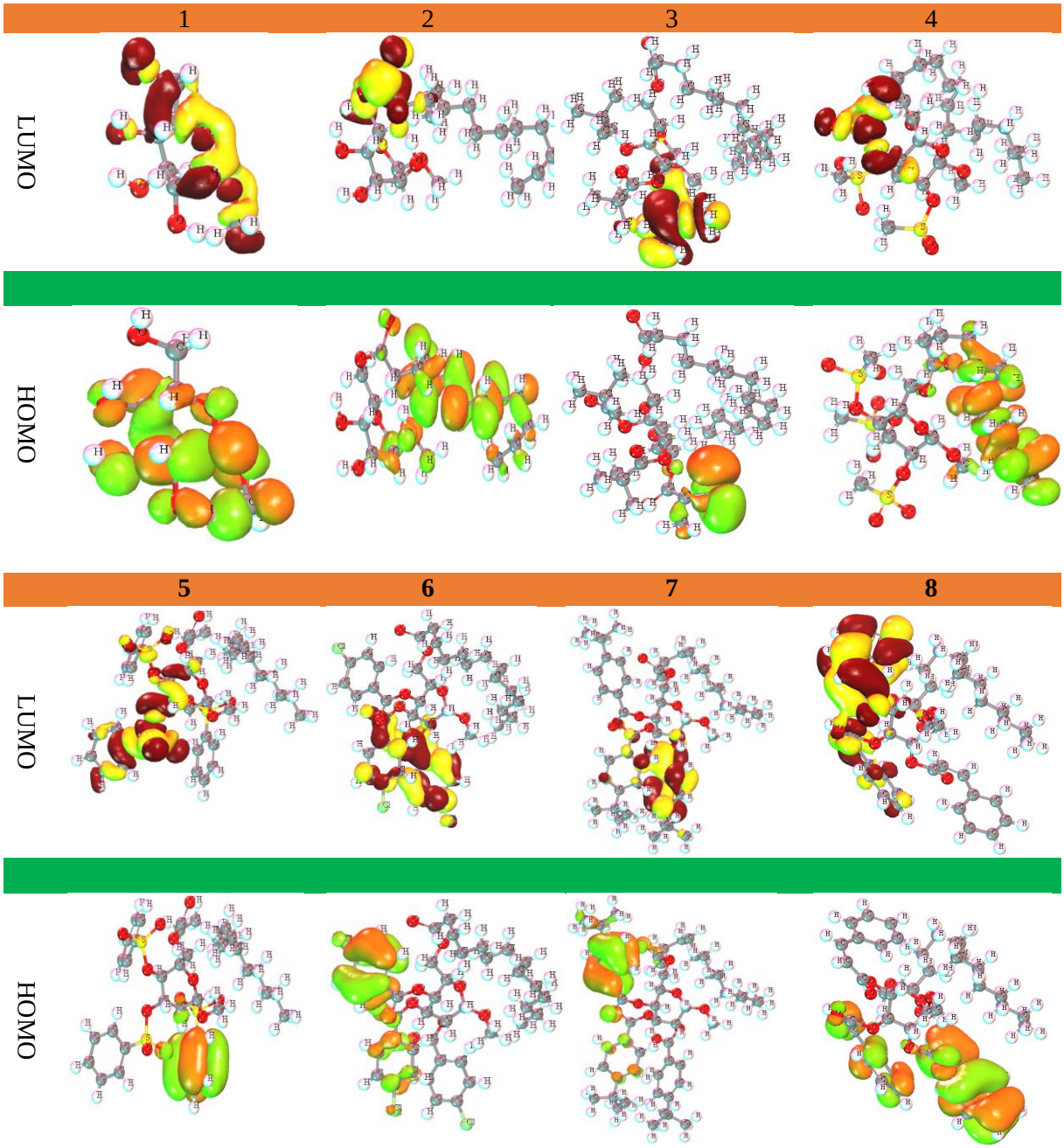

Figure 5. HOMO and LUMO picture

The positive node in HOMO is expressed by the deep green and the negative node is marked by the radish hue. In the case of LUMO, the yellow color shows the negative portion of the orbital, whereas the lightest maroon color represents the positive part of the orbital. With a specific-colored image Figure

5, all additional molecules may be found and accessed. According to the results, it appears that HOMO is located at the terminal of a benzene ring, which could describe the aromatic ring resonance phenomenon. The prevalence of oxygen atoms is generated by the existence of LUMO and the benzene ring and alkyl group indicate the HOMO.

3.8. Molecular Electrostatic Potential (MEP) Charge Distribution Mapping

Molecular electrostatic potential (MEP) mappings are frequently utilized enabling qualitative assessments of electrophilic and nucleophilic phenomena.[59] Besides that, using Molecular electrostatic potential (MEP), ligands or protein binding regions can be obtained. Underneath Figure 6, the positive electrostatic potential area has been pointed in blue color (electrophilic site), and the red color area reported the nucleophilic binding sites.MEP maps simultaneously display molecular shape and size, with positive, negative, and neutral electrostatic probability areas indicated by differing colors, and are therefore useful for studies of correlation between compound structures and physicochemical parameters. MEPs were calculated to identify reactive zones for electrophilic and nucleophilic attack of optimized structures of compounds **1-8**.

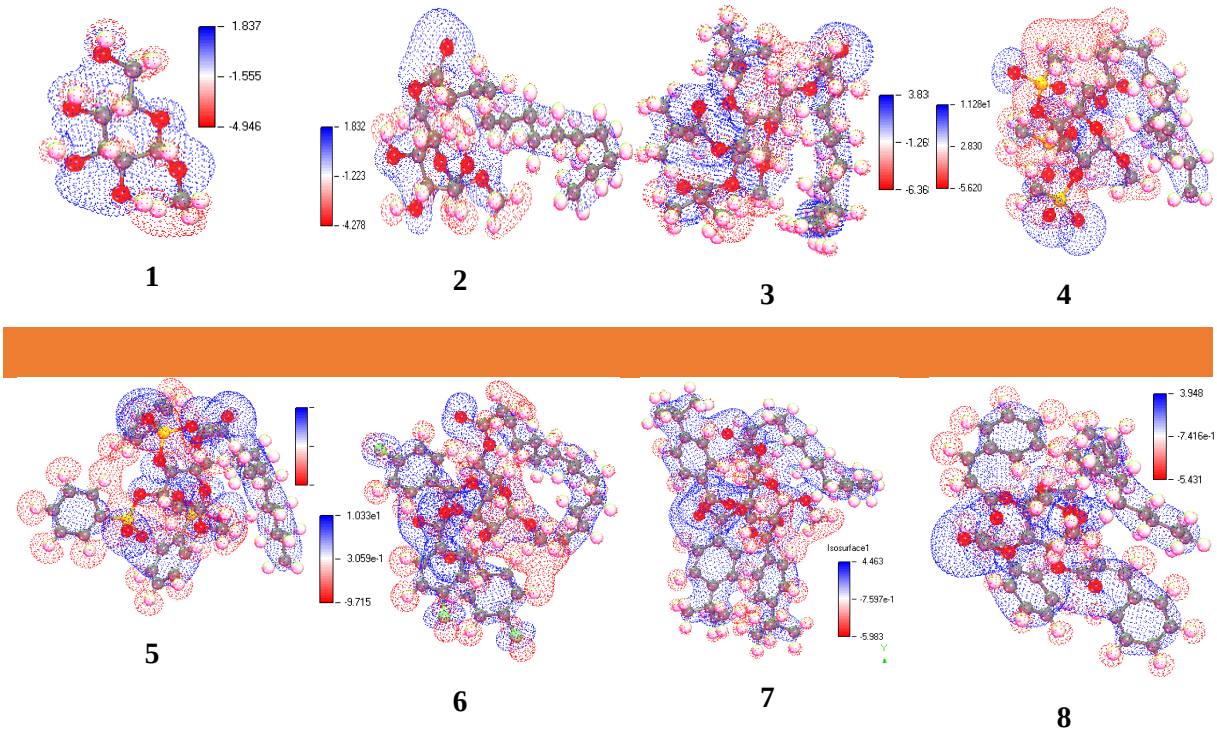

Figure 6. Molecular electrostatic potential (MEP) mappings

3.9. Molecular Docking

To find out the pathogens' protein with ligand's binding affinity; molecular docking experiments have been performed (Table 5). The active site and quantity of hydrogen bonds, hydrophobic bonds, polar and non-polar bonds, in which site of the pathogens' protein they are connected are also identified by molecular docking studies experiment. The standard binding affinity has been considered -6.0 kcal/mol.[60]Through molecular docking experiment, we have found; all the compounds have good activity as opposed to standard affinity. But the compounds 5, 6, 7 and 8 show the most biological activity among them. That's why we have proceeded to dock them with three more human pathogenic bacteria and four more human pathogenic fungi.

Table 5. Docking score against fungi and bacteria.

	Fungi and bacteria								
	***Aspergillus niger* (1ACZ) (fungi)**			***Aspergillus niger* (1KUM) (fungi)**			***Salmonella typhi* (3UU2) (bacteria)**		
Entry	**Binding Affinity (kcal/mol)**	**No of H bond**	**No of Hydrophobic bond**	**Binding Affinity (kcal/mol)**	**No of H bond**	**No of Hydrophobic bond**	**Binding Affinity (kcal/mol)**	**No of H bond**	**No of Hydrophobic bond**
1	-4.6	01	Absent	-4.7	Absent	05	-5.2	07	Absent
2	-4.9	01	18	-4.8	03	05	-5.9	05	09
3	-5.0	01	06	-5.1	06	13	-6.2	08	05
4	-5.3	03	03	-4.7	06	13	-5.7	04	03
5	-6.2	04	06	-5.2	04	21	-6.9	05	07
6	-6.6	01	05	-5.3	05	25	-7.0	10	04
7	-6.1	04	25	-4.5	04	29	-7.5	05	07
8	-5.4	04	23	-4.6	03	19	-7.0	05	03

3.10. Binding Affinities Against Human Pathogenic Bacteria

Since compound no **5**, **6**, **7** and **8** provides excellent binding affinities. That's why we selected a number of other pathogenic bacteria proteins and fungal proteins to carry out our research on a larger scale. From these, we sought to identify some specific pathogens against which our drugs would be most effective. After analyzing the docking score of the entire compound from Table 6, it is found that compound number 06 provides the highest binding energy -7.4 kcal/mol against*Salmonella enterica* (4W4M) which is slightly higher among amoxicillin and ciprofloxacin standard.

Table 6. Binding affinity for bacteria against glucopyranoside derivatives

	Tested bacteria								
	***Salmonella enterica* (4W4M)**			***Francisella tularensis* (3TQV)**			***Helicobacter pylori* (5J1L)**		
Entry	**Binding affinity (kcal/mol)**	**No. of H bond**	**No. hydrophobic Bond**	**Binding affinity (kcal/mol)**	**No. of H bond**	**No. of hydrophobic bond**	**Binding affinity (kcal/mol)**	**No, of H bond**	**No, of hydrophobic bond**
5	-7.0	07	06	-6.8	05	16	-7.0	05	03
6	-7.4	05	09	-6.7	03	18	-7.2	05	03
7	-6.2	05	05	-6.4	02	12	-7.3	02	09
8	-6.4	03	04	-7.0	03	13	-6.6	06	04
Amoxicillin	-6.8	04	04	-7.1	02	07	-6.5	04	06
Ciprofloxacin	-6.7	04	05	-7.0	03	09	-7.6	05	05

3.11. Binding Affinities Against Human Pathogenic Fungi

With starting, 08 shows the most binding affinity(-10.0 kcal/mol) against *Cryptococcus neoformans*(6KO6),and *candida albicans*(4YDE)is also bonded the highest activity by the drugs number 5, 6, and 7 (-9.4, 9.2 and -9.6 kcal/mol) (Table 7). As the -6.00 kcal/mol is the standard value to be a drug candidate. And after reviewing all of the above results, it could be concluded that the mentioned compounds can be used as antifungal drugs as opposed to fungi.

Table 7. Binding affinity analysis for fungi against glucopyranoside derivatives

	***Pneumocystis carinii* (4IXE)**			***Coccidioides immitis* (1D2K)**			***Cryptococcus neoformans* (6KO6)**			***Candida albicans* (4YDE)**		
Entry	**Binding Affinity (kcal/mol)**	**No of H bond**	**No of Hydrophobic bond**	**Binding Affinity (kcal/mol)**	**No of H bond**	**No of Hydrophobic bond**	**Binding Affinity (kcal/mol)**	**No of H bond**	**No of Hydrophobic bond**	**Binding Affinity (kcal/mol)**	**No of H bond**	**No of Hydrophobic bond**
5	-8.8	02	12	-7.7	07	14	-8.4	08	14	-9.4	10	07
6	-8.0	06	09	-8.9	04	24	-8.8	03	22	-9.2	02	13
7	-9.3	01	14	-7.2	03	09	-7.9	03	15	-9.6	05	12
8	-8.5	03	12	-8.6	04	13	-10.0	05	16	-7.8	03	07
Fluconazole	-7.3	02	08	-7.3	05	07	-7.4	05	10	-7.6	02	06
Amphotericin B	-8.5	03	09	-7.9	06	10	-7.9	04	11	-9.5	05	08

3.12. Ligand-protein Interaction and Molecular Docking Poses

Tables S1, S2, S3 represent the ligand-protein interaction with bond distance and it is found that the number of hydrogen bonds is less than hydrophobic bonds against all pathogens but the hydrogen bonds are stronger than hydrophobic bonds with respect to bond distance. It may be revealed that the hydrogen bond distance is smaller than the hydrophobic bond distance although the number is an inverse phenomenon. In addition, the different docking poses for the highest scored compound 07 have illustrated in Figure 7.

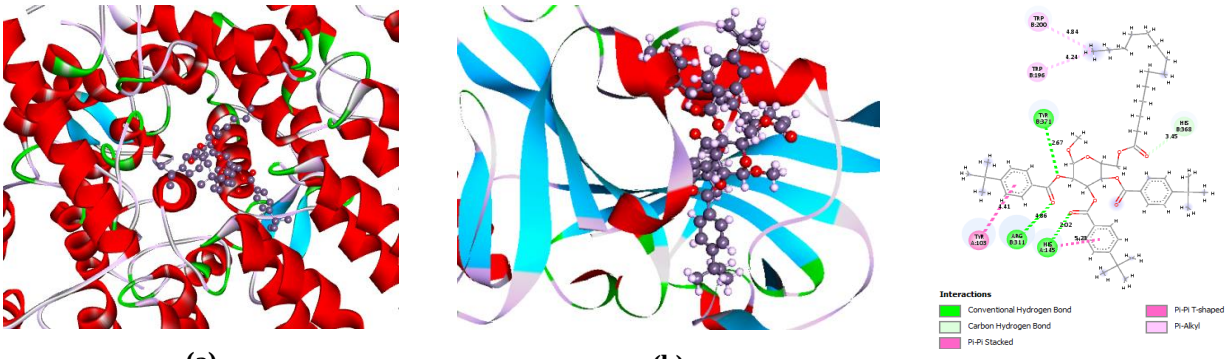

(a) **(b)** **(c)**

(Figure continued..)

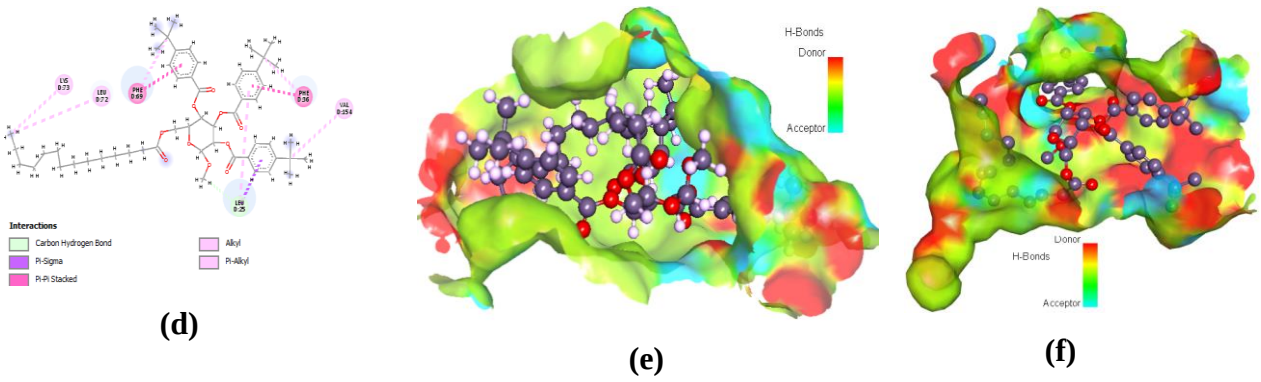

(d) **(e)** **(f)**

Figure 7. (**a**,**b**,**c,d**); Molecular docking poses of compound **7** against*Candida albicans* and *Pneumocystis carinii* and *Pneumocystis carinii*,(**e**,**f**); hydrogen bond surfaceof compound **7** against*Candida albicans* and *Pneumocystis carinii*

3.13. Molecular Dynamic Simulation

To evaluate docking correctness, molecular dynamics has been performed (Figures 8 and 9). The root means square deviation (RMSD) and root mean square fluctuation (RMSF), which give detailed information on the binding position of the ligand-protein complex when docking is completed. To achieve accurate docking, the root means square deviation (RMSD) needs to be less than 2 Å for the ligand to be properly aligned in its drug pocket.[61]By comparing the docked complex with the docked posture, RMSD is calculated. The lower number implies that the docking technique has a high degree of precision and stability.[62]Protein-ligand RMSD, ligand-protein interaction and hydrogen bonding, and ligand RMSF have been used to assess the stability of these four docked complexes. The RMSD and interactions of amino acid residues in the protein in this experiment has been determined for time (0-100 ns).

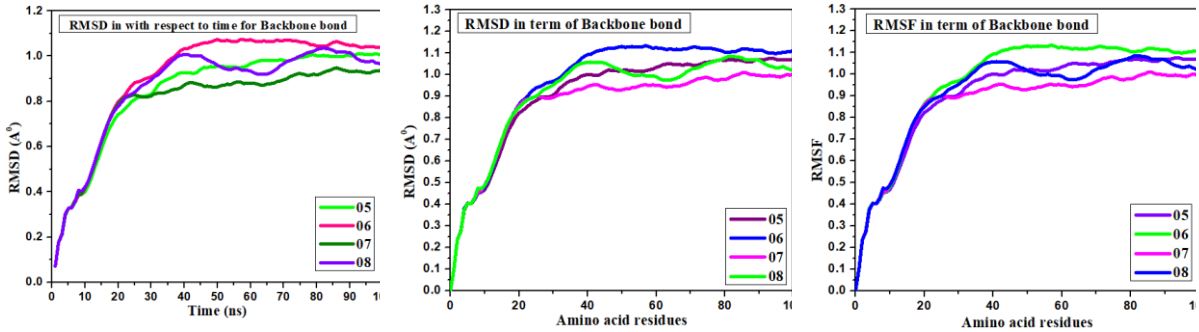

a) RMSD: Time vs protein skeleton

b) RMSD: Amino acid vs backbond

c) RMSF: Amino acid vs backbond

Figure 8. Various picture of RMSD and RMSF for protein(3UU2)

With reference to the RMSF of the docked complexes, a lower RMSF suggests more stability compare to high RMSF. The lowest RMSF of the docked complexes was found to be around 0.8 in derivatives 05 and 07, implying the best stability. The RMSD value, on the other hand, was determined to be between 0.8 to 1.0Åwhich corresponds to the standard drug.

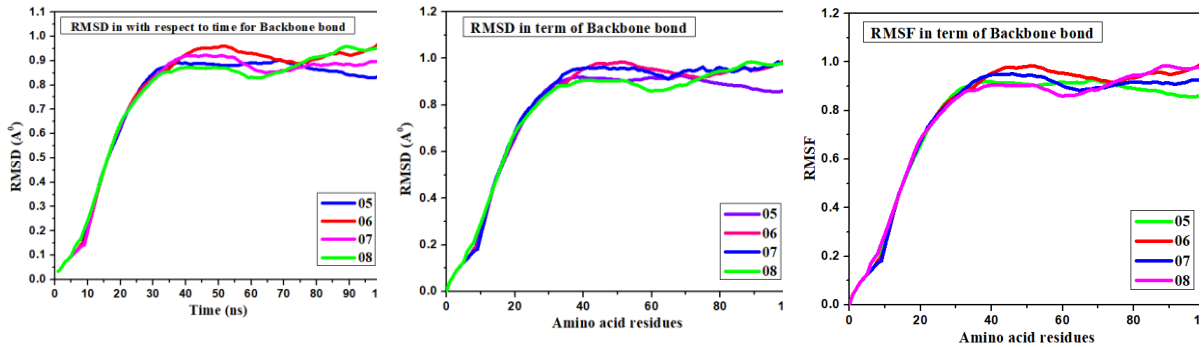

a) RMSD: Time vs protein skeleton

b) RMSD: Amino acid vs backbond

c) RMSF: Amino acid vs backbond

Figure 9. Various pictures of RMSD and RMSF for protein(5J1L)

3.14. ADME Studies

The admetSAR was performed for the prediction of drug or mentioned chemical compounds ADMET characteristics using free tool admetSAR website. A total of nine ADMET parameters have been taken which include human intestinal absorption (HIA), blood–brain barrier (BBB), Caco-2 permeability, P-I glycoprotein inhibitor, renal organic cation transporter, sub-cellular localization, CYP450 2C9 substrate, CYP450 1A2 inhibitor from AdmetSAR prediction. The results are summarized in Table 8. The results provide the information for molecules that are safer to use.

Table 8. Data for ADME parameters.

	Different parameters								
Entry	**Human Intestinal Absorption**	**Caco-2 Permeability**	**Blood Brain Barrier**	**P- I glycoprotein inhibitor**	**P- II glycoprotein substrate**	**Renal Organic Cation Transporter**	**Sub-cellular localization**	**CYP450 2C9 Substrate**	**CYP450 1A2 Inhibitor**
1	0.8373	0.8160	Yes	No	No	No	Mitochondria	No	No
2	0.6797	0.6741	Yes	No	Yes	No	Mitochondria	No	No
3	0.9013	0.5894	Yes	Yes	Yes	No	Mitochondria	No	No
4	0.9576	0.5903	Yes	Yes	No	No	Mitochondria	No	No
5	0.9412	0.5968	Yes	Yes	No	No	Mitochondria	No	No
6	0.9545	0.6289	Yes	Yes	Yes	No	Mitochondria	No	No
7	0.9452	0.6174	Yes	Yes	No	No	Mitochondria	No	No
8	0.9736	0.6888	Yes	Yes	Yes	No	Mitochondria	No	No

3.15. Aquatic and Non-aquatic Toxicity

The aquatic and non-aquatic toxicity of our finding of the tested compounds have been observed that all drugs are non-cancerogenic, non-AMES toxicity, excellent water solubility which indicates that

they have a moderate affinity to water and highly dissolving ability which means they will dissolve very rapidly while they are taken in the human body. On the other hand, all the compounds have shown different acute oral toxicity and their lowest below has been found 1.754 kg/mol where the highest was 3.258 kg/mol. *Tetrahymena pyriformis* toxicity has also been found positive excluding compound 1 (Table 9). After analysis, we have found that these compounds have no carcinogenicity properties, good water solubility and the other value is also satisfied.

Table 9. Aquatic and non-aquatic toxicity

Entry	AMES toxicity	Carcinogenicity	Water solubility, Log S	Plasma protein binding	Acute oral toxicity, kg/mol	Oral Rat acute toxicity (LD50) (mol/kg)	Fish toxicity pLC50 mg/L	*T. pyriformis* toxicity (log ug/L)
1	No	No	-0.621	0.159	2.528	1.1350	2.6152	-1.1613
2	No	No	-1.675	1.045	2.414	2.0091	1.8942	0.9370
3	No	No	-3.213	0.85	2.023	1.8904	1.1934	1.1262
4	No	No	-3.099	0.861	2.733	2.4149	1.4183	07132
5	No	No	-3.665	1.163	3.258	2.3559	1.1986	0.7558
6	No	No	-4.675	1.276	1.754	2.5098	0.0879	1.6482
7	No	No	-4.491	1.188	2.224	2.0922	0.2264	1.7552
8	No	No	-4.341	1.115	2.305	2.1551	-0.0542	1.8838

3.16. Calculation of QSAR and pIC$_{50}$

The QSAR is a computational modeling approach for revealing correlations among the structural characteristics of chemical substances and biological activity. To complete the calculated QSAR and pIC50 value, we took help from a free web tool is called Chemdesk and takes the required value including Chiv5, MRVSA9, PEOEVSA5, GATSv4, diameter etc. After that, the multiple linear regression (MLR) equations is utilized to obtain the QSAR and pIC50 value.[63] Our finding compound has been shown and meets all the criteria and different QSAR and pIC50. The range of the QSAR and pIC50 lowest value been obtained 4.19 where the highest value has obtained 7.09 (Table 10).

Table 10. Data of QSAR.

	Values								
Entry	**Chiv5**	**(bcutm1)**	**(MRVSA9)**	**(MRVSA6)**	**(PEOEVSA5)**	**GATSv4**	**J**	**Diameter**	**PIC50**
1	0.752	3.733	0.000	0.00	0.00	0.99	2.659	6	4.19
2	2.239	3.748	5.969	0.00	71.132	0.96	2.024	20.0	5.79
3	3.449	3.832	23.877	0.00	71.132	1.10	2.983	23	6.44
4	4.728	4.619	36.324	0.00	71.132	1.15	2.705	22	7.09
5	6.956	4.655	83.188	90.96	125.729	1.53	1.499	25	6.40
6	4.649	3.798	58.68	104.55	105.935	1.26	1.438	26	5.22
7	5.058	3.994	23.877	106.17	169.844	1.41	1.512	27	6.89
8	4.427	3.881	42.105	125.91	162.27	1.33	1.397	27	6.09

4. Conclusions

Recent advances in the treatment of infectious diseases have established that the use of carbohydrates could contain the effects of resistant races of microbes. In this case, a deep understanding of the antimicrobial activity mechanism is a better way which undoubtedly leads to designing new antimicrobial compounds with improved and effective activity. The literature survey revealed that most biologically active compounds contain aromatic, hetero-aromatic and acyl substituents. Benzene and its derivatives as well as nitrogen, sulfur and halogen used as substituents are known to improve the biological activity of the parent compound. In this study, various biological significance parameters through the computational tools- molecular docking by binding affinity, PASS prediction,ADME parameters, toxicity, and quantum calculation of reported derivatives (methyl α-D-glucopyranoside) have been obtained with sufficient reason and explanation. As the methyl α-D-glucopyranoside and its derivatives could show the antimicrobial activity, these are tested by binding affinity from molecular docking while all of these are highly biological significant against both bacteria and fungi but the **5**, **6**, **7** and **8** are higher than the first four compounds **8** (−10.00 kcal/mol) against *Cryptococcus neoformans*, 6KO6). In addition, compound **7** shows a higher value against fungi than bacteria even other compounds which are an almost similar phenomenon to compounds **5**, **6** and **8** which are studied discretely against four different pathogenic fungi. The quantum calculation for chemical descriptors is more supportive evidence for the computational data with giving fill-up the literature lacking chemical and biological stability and protein attacking sites. The QSAR data shows that with increasing the molecular weight and chain length, the pIC50 increases but stays below the standard. Finally, these compounds are low toxic, non-carcinogenic, satisfied the PASS predicted data and drug-likeness. In the end, it must be concluded that the compounds **5**, **6**, **7** and **8** are antifungal potential drugs while **7** is superior.

Acknowledgements

The authors are very thankful to the Research and Publication Cell, University of Chittagong, Bangladesh for providing financial support.

Supporting Information

Supporting information accompanies this paper on http://www.acgpubs.org/journal/organic-communications

ORCID ID

Sarkar M.A. Kawsar:0000-0001-7964-9117
Ajoy Kumer:0000-0001-5136-6166
Nasrin S. Munia: 0000-0002-0311-9993
Mohammed A. Hosen:0000-0002-7445-8183
Unesco Chakma:0000-0003-1711-7216
Shopnil Akash:0000-0003-1751-705X

References

[1] Slavin, J. L. Dietary fiber and body weight. *Nutrition***2005**, *21*, 411–418.
[2] Hounsome, N.; Hounsome,B.; Tomos, D.; Edwards-Jones, G. Plant metabolites and nutritional quality of vegetables. *J. Food Sci.***2008**, *73*, R48–R65.
[3] Longatte, G.; Rappaport, F.; Wollman, F-A.; Guille-Collignon M.; Lemaître, F. () Mechanism and analyses for extracting photosynthetic electrons using exogenous quinones–what makes a good extraction pathway? Photochem. *Photobiol. Sci.***2016**, *15*, 969–979.
[4] Islam, S.; Hosen, M. A.; Ahmad, S.; ul Qamar, M. T.; Dey, S.; Hasan, I.; Fujii, Y.; Ozeki, Y.; Kawsar, S. M. A. Synthesis, antimicrobial, anticancer activities, PASS prediction, molecular docking, molecular

dynamics and pharmacokinetic studies of designed methyl α-D-glucopyranoside esters. *J. Mol. Struct.***2022**, *1260*, 132761.

[5] Farhana, Y.; Amin, M. R.; Hosen, A.; Kawsar, S. M. A. Bromobenzoylation of methyl α-D-mannopyranoside: synthesis and spectral characterization. *J. Sib. Fed. Univ. Chem.***2021**, *14*, 171–183,

[6] Manninen, A. H. Metabolic effects of the very-low-carbohydrate diets: misunderstood villains of human metabolism. *J. Int. Soc. Sports Nutr.***2004**, *1*, 1–5.

[7] Amin,M. R.; Yasmin, F.; Dey, S.; Mahmud, S.; Saleh, M. A.; Emran, T. B.; Hasan, I.; Rajia, S.; Ogawa, Y.; Fujii, Y.; et al. Methyl β-D-galactopyranoside esters as potential inhibitors for SARS-CoV-2 protease enzyme: synthesis, antimicrobial, PASS, molecular docking, molecular dynamics simulations and quantum computations**.** *Glycoconjugate J.***2021**, *38*, 1–30.

[8] Hossain, F.; Andreana, P. R. Developments in carbohydrate-based cancer therapeutics. *Pharmaceuticals* **2009**, *12*, 84.

[9] Ernst, B.; Magnani, J. L. From carbohydrate leads to glycomimetic drugs. *Nature Rev. Drug Discov.***2009**, *8*, 661–677.

[10] Bielski, R.; Witczak,Z. J.; Newport, J. F. L. Carbohydrate-based micro/nanocapsules with controlled external surface for medical applications. *Frontiers Chem.***2020**, *8*, 545.

[11] Mosaiab, T.; Farr,D. C.; Kiefel,M. J.; Houston, T. A. Carbohydrate-based nanocarriers and their application to target macrophages and deliver antimicrobial agents. *Adv. Drug Delivery Rev.***2019**, *151*, 94–129.

[12] He, H.; Cao, R.; Liu,X. Y.; Li,W.; Yu, D.; Li, Y.; Liu, M.; Wu,Y.; Wu,P.; Yang, J. S.; Yan, Y.; Yang, J.; Zheng, Z. B.; Zhong, W.;Qin, Y. A light-and heat-driven glycal diazidation approach to nitrogenous carbohydrate derivatives with antiviral activity. *Org. Biomol. Chem.***2020**, *18*, 6155–6161.

[13] Ritter ,T. K.; Wong, C. H. Carbohydrate-based antibiotics: a new approach to tackling the problem of resistance. Angew. *Chem. Int. Edit.***2001**, *40*, 3508–3533.

[14] Englyst, H. N. H.; Geoffrey, J. The classification and measurement of dietary carbohydrates. *Food Chem.***1996**, *57*, 15–21.

[15] Misbah, M. M. H.; Ferdous, J.; Bulbul, M. Z. H.; Chowdhury, T. S.; Dey, S.; Hasan, I.; Kawsar, S. M. A. Evaluation of MIC, MBC, MFC and anticancer activities of acylated methyl β-D-galactopyranoside esters. *Int. J. Biosci.***2020**, *16*, 299–309.

[16] Farhana, Y.; Amin, M. R.; Hosen, M. A.; Bulbul, M. Z. H.; Dey, S.; Kawsarm S. M. A. Monosaccharide derivatives: Synthesis, antimicrobial, PASS, antiviral, and molecular docking studies against SARS-CoV-2 m^{pro} inhibitors.*J. Cellul. Chem .Technol.***2021**, *55*, 477–499.

[17] Amin, M. R.; Yasmin, F.; Hosen, M. A.; Dey, S.; Mahmud, S.; Saleh, M. A.; Hasan, I.; Fujii, Y.; Yamada, M.; Ozeki, Y.; et al. Kawsar, Synthesis, antimicrobial, anticancer, PASS, molecular docking, molecular dynamic simulations and pharmacokinetic predictions of some methyl β-D-galactopyranoside analogs**.** *Molecules***2021**, *26*, 1–25.

[18] Kawsar, S. M. A.; Kumar, A. Computational investigation of methyl α-D-glucopyranoside derivatives as inhibitor against bacteria, fungi and COVID-19 (SARS-2). *J. Chil. Chem. Soci.***2021**, *66*, 5206–5214.

[19] Kawsar, S. M. A.; Faruk, M. O.; Rahman, M. S.; Fujii, Y.; Ozeki, Y. Regioselective synthesis, characterization, and antimicrobial activities of some new monosaccharide derivatives. *Scientia. Pharm.* **2014**, *82*, 1–20.

[20] Kurtz, J. R.; Goggins, J. A.; McLachlan, J. B. () Salmonella infection: interplay between the bacteria and host immune system. *Immunol. Lett.***2017**, *190*, 42–50.

[21] Eng, S. K.; Pusparajah,P.; Mutalib,N. S. A.; Ser,H. L.; Chan,K. G.; Lee,L. H. Salmonella: a review on pathogenesis, epidemiology and antibiotic resistance. *Frontiers Life Sci.***2015**,*8*, 284–293.

[22] Chaudhury, S.; Abdulhameed, M. D. M.; Singh, N.; Tawa, G. J.; D'haeseleer, P. M.; Zemla,A. T.; Navid, A.; Zhou, C. E.; Franklin,M. C.; Cheung, J.; Rudolph, M. J.; Love, J.; Graf, J. F.; Rozak, D. A.; Dankmeyer, J. L.; Amemiya, K.; Daefler, S.; Wallqvist, A. () Rapid countermeasure discovery against Francisella tularensis based on a metabolic network reconstruction. *PLoS One.***2013**, *8*, e63369.

[23] An, D. R.; Im, H. N.; Jang, J. Y.; Kim, H. S.; Kim, J.; Yoon, H. J.; Hesek, D.; Lee, M.; Mobashery, S.; Kim,S. J.; Suh, S. W. () Structural basis of the heterodimer formation between cell shape-determining proteins Csd1 and Csd2 from Helicobacter pylori. *PloS one.***2016**, *11*, e0164243.

[24] Chander, J. Textbook of Medical Mycology. JP Medical Ltd.**2017**.

[25] García-Moreno, J.; Melendo-Pérez, S.; Martín-Gómez, M. T.; Frick, M. A.; Balcells-Ramírez, J.; Pujol-Jover, M.; Martín-Nalda, A.; Mendoza-Palomar, N.; Soler-Palacín, P. Pneumocystis jirovecii pneumonia in children. A retrospective study in a single center over three decades. Enfermedades Infec. Microb. Clin. (English ed.)**2020**, *38*, 111–118.

[26] Patel, D.; Desai, G. M.; Frases, S.; Cordero, R. J. B.; DeLeon-Rodriguez, C. M.; Eugenin, E. A.; Nosanchuk, J. D.; Martinez, L. R. Methamphetamine enhances Cryptococcus neoformans pulmonary infection and dissemination to the brain. *Mbio.***2013**, *4*, e00400–13.

[27] Pappas, P. G. Cryptococcal infections in non-HIV-infected patients. *Trans. American Clin. Climatol. Assoc.***2013**, *124*, 61–79.
[28] Fishman, J. A. Opportunistic infections-coming to the limits of immunosuppression? Cold Spring Harbor Perspectives in Medicine. **2013**, *3*, a015669.
[29] Hosen, M. A.; Alam, A.; Islam, M.; Fujii, Y.; Ozeki. Y.; Kawsar, S. M. A. Geometrical optimization, PASS prediction, molecular docking, and in silico ADMET studies of thymidine derivatives against FimH adhesin of *Escherichia coli.Bulg. Chem. Commun* **2021**, *53*, 327–342.
[30] Kumer, A.;Chakma, U.;Kawsar, S. M. A.The inhibitory effect of some natural bioactive D-glucopyranoside derivatives against SARS-CoV-2 main protease (M^{pro}) and spike protease (S^{pro})**.** *ASM Sci. J.* **2021**, *16*, 1–18.
[31] Bulbul, M. Z. H.;Hosen, M. A.; Ferdous, J.;Misbah, M. M. H.; Chowdhury, T. S.; Kawsar, S. M. A. Thermochemical, DFT study**,** physicochemical, molecular dockingand ADMET predictions of somemodified uridine derivatives**.** *Int. J. New. Chem.***2021**, *8*, 88–110.
[32] Shamsuddin, T.; Hosen, M. A.; Alam, M. S.; Emran, T. B.; Kawsar, S. M. A. Uridine derivatives: antifungal, PASS outcomes, ADME/T, drug-likeliness, molecular docking and binding energy calculations. *Med. Sci. Int. Med. J.***2021**, *10*, 1373–1386.
[33] Rana, K. M.; Maowa, J.; Alam, A.; Hosen, A.; Dey, S.; Hasan, I.; Fujii, Y.; Ozeki, Y.; Kawsar, S. M. A. In silico DFT study, molecular docking, and ADMET predictions of cytidine analogs with antimicrobial and anticancer properties. *In Silico Pharmacol.***2021**, *9*, 1–24.
[34] Alam, A.; Hosen, M. A.; Hosen. A.; Fujii, Y.; Ozeki. Y.; Kawsar, S. M. A. Synthesis, Characterization, and Molecular Docking Against a Receptor Protein FimH of Escherichia coli (4XO8) of Thymidine Derivatives.*J. Mex. Chem. Soc.***2021**, *65*, 256–276.
[35] Bulbul, M. Z. H.; Chowdhury, T. S.; Misbah, M. M. H.; Ferdous, J.; Dey, S.; Hasan, I.; Fujii, Y.; Ozeki. Y.; Kawsar, S. M. A.Synthesis of new series of pyrimidine nucleoside derivatives bearing the acyl moieties as potential antimicrobial agents. *Pharmacia***2021**, *68*, 23–34
[36] Maowa, J.;Hosen, M. A.; Alam, A.; Rana, K. M.; Fujii, Y.; Ozeki. Y.; Kawsar, S. M. A.Pharmacokinetics and molecular docking studies of uridine derivatives as SARS- COV-2 M^{pro} inhibitors*Phys. Chem. Res.***2021**, *9*, 385–412.
[37] Delley, B. Time dependent density functional theory with DMol3. *J. Phys: Cond. Matt.***2010**, *22*, 384208.
[38] Parasuraman, S. Prediction of activity spectra for substances. *J. Pharmacol. Pharmacother.***2011**, *2*, 52–53.
[39] Daina, A.; Michielin, O.; Zoete, V. () Swiss target prediction: updated data and new features for efficient prediction of protein targets of small molecules. *Nucleic Acids Res* **2019**, *47*, W357–W364.
[40] Delano, W. L. The PyMOL molecular graphics system. De-Lano Scientific, San Carlos, CA, USA, **2002**.
[41] Dallakyan, S.; Arthur, J. O. Small-molecule library screening by docking with PyRx in Chemical Biology ed: *Springer*.**2015**, 243–250.
[42] Phillips, J. C.; Braun, R.; Wang, W.; Gumbart, J.; Tajkhorshid, E.; Villa, E.; Chipot, C.; Skeel, R. D.; Kalé ,L.; Schulten, K. Scalable molecular dynamics with NAMD. *J. Comput. Chem.***2005**, *26*, 1781–1802.
[43] Skjevik, A. A.; Madej, B. D.; Dickson, C. J.; Teigen, K.; Walker, R. C.; Gould, I. R. All-atom lipid bilayer self-assembly with the AMBER and CHARMM lipid force fields. *Chem. Commun.***2015**, *51*, 4402–4405.
[44] Cheng, F. L.; Zhou, W.; Shen, Y.; Wu, J.; Liu, Z.; Lee, G.; Philip, W.; Tang, Y. admetSAR: a comprehensive source and free tool for assessment of chemical ADMET properties. *J. Chem. Inf. Model.* **2012**, *52*, 3099–105.
[45] Devi, S. R.; Jesmin, S.; Rahman, M.; Manchur, M. A.; Fujii, Y.; Kanaly, R. A.; Ozeki, Y.; Kawsar,S. M. A. Microbial efficacy and two step synthesis of uridine derivatives with spectral characterization.*Acta Pharm. Sci.* **2019**, *57*, 47–68.
[46] Kawsar, S. M. A. Hosen, M. A. An optimization and pharmacokinetic studies of some thymidine derivatives. *Turkish Comp. Theo. Chem* **2020**, *4*, 59–66.
[47] Arifuzzaman, M.; Islam, M. M.; Rahman, M. M.; Mohammad, A. R.; Kawsar, S. M. A. An efficient approach to the synthesis of thymidine derivatives containing various acyl groups: characterization and antibacterial activities. *ACTA Pharm. Sci.***2018**, *56*, 7–22.
[48] Orrego-Ruiz, J. A.; Cabanzo, R.; Mejía-Ospino, E. Study of Colombian coals using photoacoustic Fourier transform infrared spectroscopy. *Int. J. Coal Geology.***2011**, *85*, 307–310.
[49] Sohaimi, K. S. A.; Iberahim, N. I.; Ghani, A. A.; Zamrud, Z.; Heng, C. W. Ammonium adsorption-desorption using rice husk biochar. In IOP Conference Series: *Earth Environ. Sci.***2021**,*765*,012061.
[50] Lipinski, C. A. L.; Dominy, F.; Beryl, W.; Feeney, P. J. Experimental and computational approaches to estimate solubility and permeability in drug discovery and development settings. *Adv. Drug Deliv. Rev.* **1997**, *23*, 3–25.
[51] Poroikov, V. V.; Filimonov, D. A. How to acquire new biological activities in old compounds by computer prediction. *J. Computer-Aided Mol. Design.***2002**, *16*, 819–824.

[52] Mirajul, M. I.; Arifuzzaman, M.; Monjur, M. R.; Rahman, A.; Kawsar, S. M. A. Novel methyl 4,6-O-benzylidene-α-D-glucopyranoside derivatives: synthesis, structural characterization and evaluation of antibacterial activities. *Hacettepe J. Biol. Chem.***2019**, *47*, 153–164.
[53] Marinescu, M. E.; Marton, A.; Cinteza, G.; Otilia, L.; Catalin, C. Structural studies and optical nonlinear response of some pyrazole-5-ones. *Nanosci. Nanotechnol. Lett* **2015**, *7*, 846–854.
[54] Suhasini, M. S.; Gunasekaran, E.; Ramkumaar, S. G. R. Vibrational and electronic investigations, thermodynamic parameters, HOMO and LUMO analysis on Lornoxicam by density functional theory. *J. Mol. Struct.***2015**, *1100*, 116–128.
[55] Parr, R. G. D.; Robert, A.; Levy, M.; Palke, W. E. Electronegativity: the density functional viewpoint. *J. Chem. Phys.***1978**, *68*, 3801–3807.
[56] Parr, R. G.; Szentpaly, L.; Liu, S. Electrophilicity index. *J. American Chem. Soc.***1999**, *121*, 1922–1924.
[57] Kawsar, S. M. A.; Hosen, M. A.; Chowdhury, T. S.; Rana, K. M.; Fujii, Y.; Ozeki. Y. Thermochemical, PASS, molecular docking, drug-likeness and *in silico* ADMET prediction of cytidine derivatives against HIV-1 reverse transcriptase. *Revista de Chem.***2021**, *72*, 159–178.
[58] Alam, A.; Hosen, M. A.; Islam M.; Ferdous, J.; Fujii, Y.; Ozeki. Y.; Kawsar, S. M. A. Synthesis, Antibacterial and cytotoxicity assessment of modified uridine molecules. *Curr. Adv. Chem. Biochem.* **2021**, *6*, 114–129.
[59] Deb, B. M. Force concept in chemistry. *Rev. Mod. Phys.***1973**, 45, 22.
[60] Nath, A.; Kumer, A.; Khan, M. W. Synthesis, computational and molecular docking study of some 2, 3-dihydrobenzofuran and its derivatives. *J. Mol. Struct.***2020**, *1224*, 129–225.
[61] Bertamino, A.; Iraci, N.; Ostacolo, C.; Ambrosino, P.; Musella, S.; Sarno, V. D.; Ciaglia, T.; Pepe, G.; Sala, M.; Soldovieri, M. V.; Mosca, I.; Gonzalez-Rodriguez, S.; Fernandez-Carvajal, A.; Ferrer-Montiel, A.; Novellino, E.; Taglialatela, M.; Campiglia, P.; Gomez-Monterrey, I. Identification of a potent tryptophan-based TRPM8 antagonist with in vivo analgesic activity. *J. Med. Chem.***2018**, *61*, 6140–6152.
[62] Guterres, H.; Wonpil, I. Improving protein-ligand docking results with high-throughput molecular dynamics simulations. *J. Chem. Inform. Model.***2020**, *60*, 2189–2198.
[63] Oliveira, D. B. D.; Gaudio, A. C. BuildQSAR: a new computer program for QSAR analysis. Quantitative Structure-Activity Relationships: An International Journal Devoted to Fundamental and Practical Aspects of Electroanalysis. *Mol. Inform.***2000**, *19*, 599–601.

A C G
publications
© 2022 ACG Publications